*BABAR*-PUB-01/01
SLAC-PUB-8777
hep-ex/0102030

# Measurement of *CP*-Violating Asymmetries in $B^0$ Decays to *CP* Eigenstates

## The *BABAR* Collaboration

B. Aubert,[1] D. Boutigny,[1] I. De Bonis,[1] J.-M. Gaillard,[1] A. Jeremie,[1] Y. Karyotakis,[1] J.P. Lees,[1] P. Robbe,[1] V. Tisserand,[1] A. Palano,[2] G.P. Chen,[3] J.C. Chen,[3] N.D. Qi,[3] G. Rong,[3] P. Wang,[3] Y.S. Zhu,[3] G. Eigen,[4] P.L. Reinertsen,[4] B. Stugu,[4] B. Abbott,[5] G.S. Abrams,[5] A.W. Borgland,[5] A.B. Breon,[5] D.N. Brown,[5] J. Button-Shafer,[5] R.N. Cahn,[5] A.R. Clark,[5] S. Dardin,[5] C. Day,[5] S.F. Dow,[5] T. Elioff,[5] Q. Fan,[5] I. Gaponenko,[5] M.S. Gill,[5] F.R. Goozen,[5] S.J. Gowdy,[5] A. Gritsan,[5] Y. Groysman,[5] R.G. Jacobsen,[5] R.C. Jared,[5] R.W. Kadel,[5] J. Kadyk,[5] A. Karcher,[5] L.T. Kerth,[5] I. Kipnis,[5] S. Kluth,[5] Yu.G. Kolomensky,[5] J. F. Kral,[5] R. Lafever,[5] C. LeClerc,[5] M.E. Levi,[5] S.A. Lewis,[5] C. Lionberger,[5] T. Liu,[5] M. Long,[5] G. Lynch,[5] M. Marino,[5] K. Marks,[5] A.B. Meyer,[5] A. Mokhtarani,[5] M. Momayezi,[5] M. Nyman,[5] P.J. Oddone,[5] J. Ohnemus,[5] D. Oshatz,[5] S. Patton,[5] A. Perazzo,[5] C. Peters,[5] W. Pope,[5] M. Pripstein,[5] D.R. Quarrie,[5] J.E. Rasson,[5] N.A. Roe,[5] A. Romosan,[5] M.T. Ronan,[5] V.G. Shelkov,[5] R. Stone,[5] A.V. Telnov,[5] H. von der Lippe,[5] T. Weber,[5] W.A. Wenzel,[5] M.S. Zisman,[5] P.G. Bright-Thomas,[6] T.J. Harrison,[6] C.M. Hawkes,[6] A. Kirk,[6] D.J. Knowles,[6] S.W. O'Neale,[6] A.T. Watson,[6] N.K. Watson,[6] T. Deppermann,[7] H. Koch,[7] J. Krug,[7] M. Kunze,[7] B. Lewandowski,[7] K. Peters,[7] H. Schmuecker,[7] M. Steinke,[7] J.C. Andress,[8] N.R. Barlow,[8] W. Bhimji,[8] N. Chevalier,[8] P.J. Clark,[8] W.N. Cottingham,[8] N. De Groot,[8] N. Dyce,[8] B. Foster,[8] A. Mass,[8] J.D. McFall,[8] D. Wallom,[8] F.F. Wilson,[8] K. Abe,[9] C. Hearty,[9] T.S. Mattison,[9] J.A. McKenna,[9] D. Thiessen,[9] B. Camanzi,[10] S. Jolly,[10] A.K. McKemey,[10] J. Tinslay,[10] V.E. Blinov,[11] A.D. Bukin,[11] D.A. Bukin,[11] A.R. Buzykaev,[11] M.S. Dubrovin,[11] V.B. Golubev,[11] V.N. Ivanchenko,[11] G.M. Kolachev,[11] A.A. Korol,[11] E.A. Kravchenko,[11] A.P. Onuchin,[11] A.A. Salnikov,[11] S.I. Serednyakov,[11] Yu.I. Skovpen,[11] V.I. Telnov,[11] A.N. Yushkov,[11] A.J. Lankford,[12] M. Mandelkern,[12] S. McMahon,[12] D.P. Stoker,[12] A. Ahsan,[13] C. Buchanan,[13] S. Chun,[13] D.B. MacFarlane,[14] S. Prell,[14] Sh. Rahatlou,[14] G. Raven,[14] V. Sharma,[14] S. Burke,[15] C. Campagnari,[15] B. Dahmes,[15] D. Hale,[15] P.A. Hart,[15] N. Kuznetsova,[15] S. Kyre,[15] S.L. Levy,[15] O. Long,[15] A. Lu,[15] J.D. Richman,[15] W. Verkerke,[15] M. Witherell,[15] S. Yellin,[15] J. Beringer,[16] D.E. Dorfan,[16] A.M. Eisner,[16] A. Frey,[16] A.A. Grillo,[16] M. Grothe,[16] C.A. Heusch,[16] R.P. Johnson,[16] W. Kroeger,[16] W.S. Lockman,[16] T. Pulliam,[16] H. Sadrozinski,[16] T. Schalk,[16] R.E. Schmitz,[16] B.A. Schumm,[16] A. Seiden,[16] E.N. Spencer,[16] M. Turri,[16] W. Walkowiak,[16] D.C. Williams,[16] E. Chen,[17] G.P. Dubois-Felsmann,[17] A. Dvoretskii,[17] J.E. Hanson,[17] D.G. Hitlin,[17] S. Metzler,[17] J. Oyang,[17] F.C. Porter,[17] A. Ryd,[17] A. Samuel,[17] M. Weaver,[17] S. Yang,[17] R.Y. Zhu,[17] S. Devmal,[18] T.L. Geld,[18] S. Jayatilleke,[18] S.M. Jayatilleke,[18] G. Mancinelli,[18] B.T. Meadows,[18] M.D. Sokoloff,[18] P. Bloom,[19] S. Fahey,[19] W.T. Ford,[19] F. Gaede,[19] W.C. van Hoek,[19] D.R. Johnson,[19] A.K. Michael,[19] U. Nauenberg,[19] A. Olivas,[19] H. Park,[19] P. Rankin,[19] J. Roy,[19] S. Sen,[19] J.G. Smith,[19] D.L. Wagner,[19] J. Blouw,[20] J.L. Harton,[20] M. Krishnamurthy,[20] A. Soffer,[20] W.H. Toki,[20] D.W. Warner,[20] R.J. Wilson,[20] J. Zhang,[20] T. Brandt,[21] J. Brose,[21] T. Colberg,[21] G. Dahlinger,[21] M. Dickopp,[21] R.S. Dubitzky,[21] P. Eckstein,[21] H. Futterschneider,[21] R. Krause,[21] E. Maly,[21] R. Müller-Pfefferkorn,[21] S. Otto,[21] K.R. Schubert,[21] R. Schwierz,[21] B. Spaan,[21] L. Wilden,[21] L. Behr,[22] D. Bernard,[22] G.R. Bonneaud,[22] F. Brochard,[22] J. Cohen-Tanugi,[22] S. Ferrag,[22] G. Fouque,[22] F. Gastaldi,[22] P. Matricon,[22] P. Mora de Freitas,[22] C. Renard,[22] E. Roussot,[22] S. T'Jampens,[22] C. Thiebaux,[22] G. Vasileiadis,[22] M. Verderi,[22] A. Anjomshoaa,[23] R. Bernet,[23] F. Di Lodovico,[23] A. Khan,[23] F. Muheim,[23] S. Playfer,[23] J.E. Swain,[23] M. Falbo,[24] C. Bozzi,[25] S. Dittongo,[25] M. Folegani,[25] L. Piemontese,[25] E. Treadwell,[26] F. Anulli,[27,*] R. Baldini-Ferroli,[27] A. Calcaterra,[27] R. de Sangro,[27] D. Falciai,[27] G. Finocchiaro,[27] P. Patteri,[27] I.M. Peruzzi,[27,*] M. Piccolo,[27] Y. Xie,[27] A. Zallo,[27] S. Bagnasco,[28] A. Buzzo,[28] R. Contri,[28] G. Crosetti,[28] M. Lo Vetere,[28] M. Macri,[28] M.R. Monge,[28] M. Pallavicini,[28] S. Passaggio,[28] F.C. Pastore,[28] C. Patrignani,[28] M.G. Pia,[28]

E. Robutti,[28] A. Santroni,[28] M. Morii,[29] R. Bartoldus,[30] T. Dignan,[30] R. Hamilton,[30] U. Mallik,[30] J. Cochran,[31] H.B. Crawley,[31] P.A. Fischer,[31] J. Lamsa,[31] R. McKay,[31] W.T. Meyer,[31] E.I. Rosenberg,[31] J.N. Albert,[32] C. Beigbeder,[32] M. Benkebil,[32] D. Breton,[32] R. Cizeron,[32] S. Du,[32] G. Grosdidier,[32] C. Hast,[32] A. Höcker,[32] V. LePeltier,[32] A.M. Lutz,[32] S. Plaszczynski,[32] M.H. Schune,[32] S. Trincaz-Duvoid,[32] K. Truong,[32] A. Valassi,[32] G. Wormser,[32] R.M. Bionta,[33] V. Brigljević,[33] A. Brooks,[33] O. Fackler,[33] D. Fujino,[33] D.J. Lange,[33] M. Mugge,[33] T.G. O'Connor,[33] B. Pedrotti,[33] X. Shi,[33] K. van Bibber,[33] T.J. Wenaus,[33] D.M. Wright,[33] C.R. Wuest,[33] B. Yamamoto,[33] M. Carroll,[34] J.R. Fry,[34] E. Gabathuler,[34] R. Gamet,[34] M. George,[34] M. Kay,[34] D.J. Payne,[34] R.J. Sloane,[34] C. Touramanis,[34] M.L. Aspinwall,[35] D.A. Bowerman,[35] P.D. Dauncey,[35] U. Egede,[35] I. Eschrich,[35] N.J.W. Gunawardane,[35] R. Martin,[35] J.A. Nash,[35] D.R. Price,[35] P. Sanders,[35] D. Smith,[35] D.E. Azzopardi,[36] J.J. Back,[36] P. Dixon,[36] P.F. Harrison,[36] D. Newman-Coburn,[36] R.J.L. Potter,[36] H.W. Shorthouse,[36] P. Strother,[36] P.B. Vidal,[36] M.I. Williams,[36] G. Cowan,[37] S. George,[37] M.G. Green,[37] A. Kurup,[37] C.E. Marker,[37] P. McGrath,[37] T.R. McMahon,[37] F. Salvatore,[37] I. Scott,[37] G. Vaitsas,[37] D. Brown,[38] C.L. Davis,[38] K. Ford,[38] Y. Li,[38] J. Pavlovich,[38] J. Allison,[39] R. J. Barlow,[39] J. T. Boyd,[39] J. Fullwood,[39] F. Jackson,[39] G.D. Lafferty,[39] N. Savvas,[39] E.T. Simopoulos,[39] R.J. Thompson,[39] J.H. Weatherall,[39] R. Bard,[40] A. Farbin,[40] A. Jawahery,[40] V. Lillard,[40] J. Olsen,[40] D.A. Roberts,[40] J.R. Schieck,[40] G. Blaylock,[41] C. Dallapiccola,[41] K.T. Flood,[41] S.S. Hertzbach,[41] R. Kofler,[41] C.S. Lin,[41] H. Staengle,[41] S. Willocq,[41] J. Wittlin,[41] B. Brau,[42] R. Cowan,[42] G. Sciolla,[42] F. Taylor,[42] R.K. Yamamoto,[42] D.I. Britton,[43] M. Milek,[43] P.M. Patel,[43] J. Trischuk,[43] F. Lanni,[44] F. Palombo,[44] J.M. Bauer,[45] M. Booke,[45] L. Cremaldi,[45] V. Eschenberg,[45] R. Kroeger,[45] M. Reep,[45] J. Reidy,[45] D.A. Sanders,[45] D.J. Summers,[45] M. Beaulieu,[46] J.P. Martin,[46] J.Y. Nief,[46] R. Seitz,[46] P. Taras,[46] V. Zacek,[46] H. Nicholson,[47] C.S. Sutton,[47] N. Cavallo,[48,†] C. Cartaro,[48] G. De Nardo,[48] F. Fabozzi,[48] C. Gatto,[48] L. Lista,[48] P. Paolucci,[48] D. Piccolo,[48] C. Sciacca,[48] J.M. LoSecco,[49] J.R.G. Alsmiller,[50] T.A. Gabriel,[50] T. Handler,[50] J. Heck,[50] J.E. Brau,[51] R. Frey,[51] M. Iwasaki,[51] N.B. Sinev,[51] D. Strom,[51] E. Borsato,[52] F. Colecchia,[52] F. Dal Corso,[52] F. Galeazzi,[52] M. Margoni,[52] M. Marzolla,[52] G. Michelon,[52] M. Morandin,[52] M. Posocco,[52] M. Rotondo,[52] F. Simonetto,[52] R. Stroili,[52] E. Torassa,[52] C. Voci,[52] P. Bailly,[53] M. Benayoun,[53] H. Briand,[53] J. Chauveau,[53] P. David,[53] C. De la Vaissière,[53] L. Del Buono,[53] J.F. Genat,[53] O. Hamon,[53] F. Le Diberder,[53] H. Lebbolo,[53] Ph. Leruste,[53] J. Lory,[53] L. Martin,[53] L. Roos,[53] J. Stark,[53] S. Versillé,[53] B. Zhang,[53] P.F. Manfredi,[54] L. Ratti,[54] V. Re,[54] V. Speziali,[54] E.D. Frank,[55] L. Gladney,[55] Q.H. Guo,[55] J.H. Panetta,[55] C. Angelini,[56] G. Batignani,[56] S. Bettarini,[56] M. Bondioli,[56] F. Bosi,[56] M. Carpinelli,[56] F. Forti,[56] M.A. Giorgi,[56] A. Lusiani,[56] F. Martinez-Vidal,[56] M. Morganti,[56] N. Neri,[56] E. Paoloni,[56] M. Rama,[56] G. Rizzo,[56] F. Sandrelli,[56] G. Simi,[56] G. Triggiani,[56] J. Walsh,[56] M. Haire,[57] D. Judd,[57] K. Paick,[57] L. Turnbull,[57] D.E. Wagoner,[57] J. Albert,[58] C. Bula,[58] R. Fernholz,[58] C. Lu,[58] K.T. McDonald,[58] V. Miftakov,[58] B. Sands,[58] S.F. Schaffner,[58] A.J.S. Smith,[58] A. Tumanov,[58] E.W. Varnes,[58] F. Bronzini,[59] A. Buccheri,[59] C. Bulfon,[59] G. Cavoto,[59] D. del Re,[59] R. Faccini,[14,59] F. Ferrarotto,[59] F. Ferroni,[59] K. Fratini,[59] E. Lamanna,[59] E. Leonardi,[59] M.A. Mazzoni,[59] S. Morganti,[59] G. Piredda,[59] F. Safai Tehrani,[59] M. Serra,[59] C. Voena,[59] R. Waldi,[60] P.F. Jacques,[61] M. Kalelkar,[61] R.J. Plano,[61] T. Adye,[62] B. Claxton,[62] B. Franek,[62] S. Galagedera,[62] N.I. Geddes,[62] G.P. Gopal,[62] J. Lidbury,[62] S.M. Xella,[62] R. Aleksan,[63] P. Besson,[63,‡] P. Bourgeois,[63] G. De Domenico,[63] S. Emery,[63] A. Gaidot,[63] S.F. Ganzhur,[63] L. Gosset,[63] G. Hamel de Monchenault,[63] W. Kozanecki,[63] M. Langer,[63] G.W. London,[63] B. Mayer,[63] B. Serfass,[63] G. Vasseur,[63] C. Yeche,[63] M. Zito,[63] N. Copty,[64] M.V. Purohit,[64] H. Singh,[64] F.X. Yumiceva,[64] I. Adam,[65] P.L. Anthony,[65] D. Aston,[65] K. Baird,[65] J. Bartelt,[65] J. Becla,[65] R. Bell,[65] E. Bloom,[65] C.T. Boeheim,[65] A.M. Boyarski,[65] R.F. Boyce,[65] F. Bulos,[65] W. Burgess,[65] B. Byers,[65] G. Calderini,[65] R. Claus,[65] M.R. Convery,[65] R. Coombes,[65] L. Cottrell,[65] D.P. Coupal,[65] D.H. Coward,[65] W.W. Craddock,[65] H. DeStaebler,[65] J. Dorfan,[65] M. Doser,[65] W. Dunwoodie,[65] S. Ecklund,[65] T.H. Fieguth,[65] R.C. Field,[65] D.R. Freytag,[65] T. Glanzman,[65] G.L. Godfrey,[65] P. Grosso,[65] G. Haller,[65] A. Hanushevsky,[65] J. Harris,[65] A. Hasan,[65] J.L. Hewett,[65] T. Himel,[65] M.E. Huffer,[65] W.R. Innes,[65] C.P. Jessop,[65] H. Kawahara,[65] L. Keller,[65] M.H. Kelsey,[65] P. Kim,[65] L.A. Klaisner,[65] M.L. Kocian,[65] H.J. Krebs,[65] P.F. Kunz,[65] U. Langenegger,[65] W. Langeveld,[65] D.W.G.S. Leith,[65] S.K. Louie,[65] S. Luitz,[65] V. Luth,[65] H.L. Lynch,[65] J. MacDonald,[65] G. Manzin,[65] H. Marsiske,[65] M. McCulloch,[65] D. McShurley,[65] S. Menke,[65] R. Messner,[65] S. Metcalfe,[65] K.C. Moffeit,[65] R. Mount,[65] D.R. Muller,[65] D. Nelson,[65] M. Nordby,[65] C.P. O'Grady,[65] F.G. O'Neill,[65] G. Oxoby,[65] T. Pavel,[65] J. Perl,[65] S. Petrak,[65] G. Putallaz,[65] H. Quinn,[65] P.E. Raines,[65] B.N. Ratcliff,[65] R. Reif,[65] S.H. Robertson,[65] L.S. Rochester,[65] A. Roodman,[65] J.J. Russell,[65] L. Sapozhnikov,[65] O.H. Saxon,[65] T. Schietinger,[65] R.H. Schindler,[65] J. Schwiening,[65] J.T. Seeman,[65] V.V. Serbo,[65] K. Skarpass Sr.,[65] A. Snyder,[65] A. Soha,[65] S.M. Spanier,[65] A. Stahl,[65] J. Stelzer,[65] D. Su,[65] M.K. Sullivan,[65] M. Talby,[65]

H.A. Tanaka,[65] J. Va'vra,[65] S.R. Wagner,[65] A.J.R. Weinstein,[65] J.L. White,[65] U. Wienands,[65] W.J. Wisniewski,[65] C.C. Young,[65] G. Zioulas,[65] P.R. Burchat,[66] C.H. Cheng,[66] D. Kirkby,[66] T.I. Meyer,[66] C. Roat,[66] A. De Silva,[67] R. Henderson,[67] S. Berridge,[68] W. Bugg,[68] H. Cohn,[68] E. Hart,[68] A.W. Weidemann,[68] T. Benninger,[69] J.M. Izen,[69] I. Kitayama,[69] X.C. Lou,[69] M. Turcotte,[69] F. Bianchi,[70] M. Bona,[70] B. Di Girolamo,[70] D. Gamba,[70] A. Smol,[70] D. Zanin,[70] L. Bosisio,[71] G. Della Ricca,[71] L. Lanceri,[71] A. Pompili,[71] P. Poropat,[71] G. Vuagnin,[71] R.S. Panvini,[72] C.M. Brown,[73] R. Kowalewski,[73] J.M. Roney,[73] H.R. Band,[74] E. Charles,[74] S. Dasu,[74] P. Elmer,[74] H. Hu,[74] J.R. Johnson,[74] J. Nielsen,[74] W. Orejudos,[74] Y. Pan,[74] R. Prepost,[74] I.J. Scott,[74] J.H. von Wimmersperg-Toeller,[74] S.L. Wu,[74] Z. Yu,[74] H. Zobernig,[74] T.M.B. Kordich,[75] T.B. Moore,[75] and H. Neal[75]

[1] *Laboratoire de Physique des Particules, F-74941 Annecy-le-Vieux, France*
[2] *Università di Bari, Dipartimento di Fisica and INFN, I-70126 Bari, Italy*
[3] *Institute of High Energy Physics, Beijing 100039, China*
[4] *University of Bergen, Inst. of Physics, N-5007 Bergen, Norway*
[5] *Lawrence Berkeley National Laboratory and University of California, Berkeley, CA 94720, USA*
[6] *University of Birmingham, Birmingham B15 2TT, UK*
[7] *Ruhr Universität Bochum, Inst. f. Experimentalphysik 1, D-44780 Bochum, Germany*
[8] *University of Bristol, Bristol BS8 1TL, UK*
[9] *University of British Columbia, Vancouver, BC V6T 1Z1, Canada*
[10] *Brunel University, Uxbridge, Middlesex UB8 3PH, UK*
[11] *Budker Institute of Nuclear Physics, Novosibirsk 630090, Russia*
[12] *University of California at Irvine, Irvine, CA 92697, USA*
[13] *University of California at Los Angeles, Los Angeles, CA 90024, USA*
[14] *University of California at San Diego, La Jolla, CA 92093, USA*
[15] *University of California at Santa Barbara, Santa Barbara, CA 93106, USA*
[16] *University of California at Santa Cruz, Institute for Particle Physics, Santa Cruz, CA 95064, USA*
[17] *California Institute of Technology, Pasadena, CA 91125, USA*
[18] *University of Cincinnati, Cincinnati, OH 45221, USA*
[19] *University of Colorado, Boulder, CO 80309, USA*
[20] *Colorado State University, Fort Collins, CO 80523, USA*
[21] *Technische Universität Dresden, Inst. f. Kern-u. Teilchenphysik, D-01062 Dresden, Germany*
[22] *Ecole Polytechnique, F-91128 Palaiseau, France*
[23] *University of Edinburgh, Edinburgh EH9 3JZ, UK*
[24] *Elon College, Elon College, NC 27244-2010, USA*
[25] *Università di Ferrara, Dipartimento di Fisica and INFN, I-44100 Ferrara, Italy*
[26] *Florida A&M University, Tallahassee, FL 32307, USA*
[27] *Laboratori Nazionali di Frascati dell'INFN, I-00044 Frascati, Italy*
[28] *Università di Genova, Dipartimento di Fisica and INFN, I-16146 Genova, Italy*
[29] *Harvard University, Cambridge, MA 02138, USA*
[30] *University of Iowa, Iowa City, IA 52242-3160, USA*
[31] *Iowa State University, Ames, IA 50011, USA*
[32] *Laboratoire de l'Accélérateur Linéaire, F-91898 Orsay, France*
[33] *Lawrence Livermore National Laboratory, Livermore, CA 94550, USA*
[34] *University of Liverpool, Liverpool L69 3BX, UK*
[35] *University of London, Imperial College, London SW7 2BW, UK*
[36] *Queen Mary, University of London, London E1 4NS, UK*
[37] *University of London, Royal Holloway and Bedford New College, Egham, Surrey TW20 0EX, UK*
[38] *University of Louisville, Louisville, KY 40292, USA*
[39] *University of Manchester, Manchester M13 9PL, UK*
[40] *University of Maryland, College Park, MD 20742, USA*
[41] *University of Massachusetts, Amherst, MA 01003, USA*
[42] *Massachusetts Institute of Technology, Lab for Nuclear Science, Cambridge, MA 02139, USA*
[43] *McGill University, Montréal, QC H3A 2T8, Canada*
[44] *Università di Milano, Dipartimento di Fisica and INFN, I-20133 Milano, Italy*
[45] *University of Mississippi, University, MS 38677, USA*
[46] *Université de Montréal, Lab. René J. A. Lévesque, Montréal, QC H3C 3J7, Canada*
[47] *Mount Holyoke College, South Hadley, MA 01075, USA*
[48] *Università di Napoli Federico II, Dipartimento di Scienze Fisiche and INFN, I-80126 Napoli, Italy*
[49] *University of Notre Dame, Notre Dame, IN 46556, USA*
[50] *Oak Ridge National Laboratory, Oak Ridge, TN 37831, USA*
[51] *University of Oregon, Eugene, OR 97403, USA*
[52] *Università di Padova, Dipartimento di Fisica and INFN, I-35131 Padova, Italy*
[53] *Universités Paris VI et VII, Lab de Physique Nucléaire H. E., F-75252 Paris, France*
[54] *Università di Pavia, Dipartimento di Elettronica and INFN, I-27100 Pavia, Italy*

[55] University of Pennsylvania, Philadelphia, PA 19104, USA
[56] Università di Pisa, Scuola Normale Superiore, and INFN, I-56010 Pisa, Italy
[57] Prairie View A&M University, Prairie View, TX 77446, USA
[58] Princeton University, Princeton, NJ 08544, USA
[59] Università di Roma La Sapienza, Dipartimento di Fisica and INFN, I-00185 Roma, Italy
[60] Universität Rostock, D-18051 Rostock, Germany
[61] Rutgers University, New Brunswick, NJ 08903, USA
[62] Rutherford Appleton Laboratory, Chilton, Didcot, Oxon OX11 0QX, UK
[63] DAPNIA, Commissariat à l'Energie Atomique/Saclay, F-91191 Gif-sur-Yvette, France
[64] University of South Carolina, Columbia, SC 29208, USA
[65] Stanford Linear Accelerator Center, Stanford, CA 94309, USA
[66] Stanford University, Stanford, CA 94305-4060, USA
[67] TRIUMF, Vancouver, BC V6T 2A3, Canada
[68] University of Tennessee, Knoxville, TN 37996, USA
[69] University of Texas at Dallas, Richardson, TX 75083, USA
[70] Università di Torino, Dipartimento di Fisica Sperimentale and INFN, I-10125 Torino, Italy
[71] Università di Trieste, Dipartimento di Fisica and INFN, I-34127 Trieste, Italy
[72] Vanderbilt University, Nashville, TN 37235, USA
[73] University of Victoria, Victoria, BC V8W 3P6, Canada
[74] University of Wisconsin, Madison, WI 53706, USA
[75] Yale University, New Haven, CT 06511, USA

(Dated: February 18, 2001)

We present measurements of time-dependent $CP$-violating asymmetries in neutral $B$ decays to several $CP$ eigenstates. The measurement uses a data sample of 23 million $\Upsilon(4S) \to B\overline{B}$ decays collected by the *BABAR* detector at the PEP-II asymmetric $B$ Factory at SLAC. In this sample, we find events where one neutral $B$ meson is fully reconstructed in a $CP$ eigenstate containing charmonium and the flavor of the other neutral $B$ meson is determined from its decay products. The amplitude of the $CP$-violating asymmetry, which in the Standard Model is proportional to $\sin 2\beta$, is derived from the decay time distributions in such events. The result is $\sin 2\beta = 0.34 \pm 0.20$ (stat) $\pm 0.05$ (syst).

PACS numbers: 13.25.Hw, 12.15.Hh, 11.30.Er

$CP$-violating asymmetries in the time distributions for decays of $B^0$ and $\overline{B}^0$ mesons provide a direct test of the Standard Model of electroweak interactions [1]. For the neutral $B$ decay modes reported here, corrections to $CP$-violating effects from strong interactions are absent, in contrast to the $K^0_L$ modes in which $CP$ violation was discovered [2].

Using a data sample of 23 million $B\overline{B}$ pairs recorded at the $\Upsilon(4S)$ resonance by the *BABAR* detector at the PEP-II asymmetric-energy $e^+e^-$ collider at the Stanford Linear Accelerator Center, we have fully reconstructed a sample $B_{CP}$ of neutral $B$ mesons decaying to the $CP$ eigenstates $J/\psi K^0_S$, $\psi(2S)K^0_S$ and $J/\psi K^0_L$. We examine each of the events in this sample for evidence that the other neutral $B$ meson decayed as a $B^0$ or a $\overline{B}^0$, designated as a $B^0$ or $\overline{B}^0$ flavor tag. The final $B_{CP}$ sample contains about 360 signal events.

When the $\Upsilon(4S)$ decays, the $P$-wave $B\overline{B}$ state evolves coherently until one of the mesons decays. In one of four time-order and flavor configurations, if the tagging meson $B_{\rm tag}$ decays first, and as a $B^0$, the other meson must be a $\overline{B}^0$ at that same time $t_{\rm tag}$. It then evolves independently, and can decay into a $CP$ eigenstate $B_{CP}$ at a later time $t_{CP}$. The time between the two decays $\Delta t = t_{CP} - t_{\rm tag}$ is a signed quantity made measurable by producing the $\Upsilon(4S)$ with a boost $\beta\gamma = 0.56$ along the collision ($z$) axis, with nominal energies of 9.0 and 3.1 GeV for the electron and positron beams. The measured distance $\Delta z \approx \beta\gamma c\Delta t$ between the two decay vertices provides a good estimate of the corresponding time interval $\Delta t$; the average value of $|\Delta z|$ is $\beta\gamma c\tau_{B^0} \approx 250\,\mu$m.

The decay-time distribution for events with a $B^0$ or a $\overline{B}^0$ tag can be expressed in terms of a complex parameter $\lambda$ that depends on both $B^0\overline{B}^0$ mixing and on the amplitudes describing $\overline{B}^0$ and $B^0$ decay to a common final state $f$ [3]. The distribution $\mathrm{f}_+(\mathrm{f}_-)$ of the decay rate when the tagging meson is a $B^0(\overline{B}^0)$ is given by

$$\mathrm{f}_\pm(\Delta t) = \frac{\mathrm{e}^{-|\Delta t|/\tau_{B^0}}}{2\tau_{B^0}(1+|\lambda|^2)} \times \left[ \frac{1+|\lambda|^2}{2} \pm \mathcal{I}m\lambda \sin(\Delta m_{B^0}\Delta t) \mp \frac{1-|\lambda|^2}{2}\cos(\Delta m_{B^0}\Delta t)\right], \quad (1)$$

where $\tau_{B^0}$ is the $B^0$ lifetime and $\Delta m_{B^0}$ is the mass difference determined from $B^0\overline{B}^0$ mixing [4], and where the lifetime difference between neutral $B$ mass eigenstates is assumed to be negligible. The first oscillatory term in Eq. 1 is due to interference between direct decay and decay after mixing. A difference between the $B^0$ and $\overline{B}^0$ distributions or a $\Delta t$ asymmetry for either tag is evidence for $CP$ violation.

If all amplitudes contributing to $B^0 \to f$ have the same weak phase, a condition satisfied in the Standard Model for charmonium-containing $b \to c\overline{c}s$ decays, then $|\lambda| = 1$. For these $CP$ eigenstates the Standard Model predicts $\lambda = \eta_f e^{-2i\beta}$, where $\eta_f$ is the $CP$ eigenvalue of the state $f$ and $\beta = \arg\left[-V_{\rm cd}V_{\rm cb}^*/V_{\rm td}V_{\rm tb}^*\right]$ is an angle of the Unitarity Triangle of the three-generation Cabibbo-Kobayashi-Maskawa (CKM) matrix [5]. Thus, the time-dependent $CP$-violating asymmetry is

$$\begin{aligned} A_{CP}(\Delta t) &\equiv \frac{\mathrm{f}_+(\Delta t) - \mathrm{f}_-(\Delta t)}{\mathrm{f}_+(\Delta t) + \mathrm{f}_-(\Delta t)} \\ &= -\eta_f \sin 2\beta \sin(\Delta m_{B^0}\,\Delta t), \end{aligned} \qquad (2)$$

where $\eta_f = -1$ for $J/\psi K_S^0$ and $\psi(2S)K_S^0$ and $+1$ for $J/\psi K_L^0$.

A measurement of $A_{CP}$ requires determination of the experimental $\Delta t$ resolution and the fraction of events in which the tag assignment is incorrect. A mistag fraction $w$ reduces the observed asymmetry by a factor $(1-2w)$.

Several samples of fully reconstructed $B^0$ mesons are used in this measurement. The $B_{CP}$ sample contains candidates reconstructed in the $CP$ eigenstates $J/\psi K_S^0$ ($K_S^0 \to \pi^+\pi^-, \pi^0\pi^0$), $\psi(2S)K_S^0$ ($K_S^0 \to \pi^+\pi^-$) and $J/\psi K_L^0$. The $J/\psi$ and $\psi(2S)$ mesons are reconstructed through their decays to $e^+e^-$ and $\mu^+\mu^-$; the $\psi(2S)$ is also reconstructed through its decay to $J/\psi\pi^+\pi^-$. A sample of $B$ decays $B_{\rm flav}$ [6] used in the determination of the mistag fractions and $\Delta t$ resolution functions consists of the channels $D^{(*)-}h^+(h^+ = \pi^+, \rho^+, a_1^+)$ and $J/\psi K^{*0}$ ($K^{*0} \to K^+\pi^-$). A control sample of charged $B$ mesons decaying to the final states $J/\psi K^{(*)+}$, $\psi(2S)K^+$ and $D^{(*)0}\pi^+$ is used for validation studies.

A description of the *BABAR* detector can be found in Ref. [7]. Charged particles are detected and their momenta measured by a combination of a silicon vertex tracker (SVT) consisting of five double-sided layers and a central drift chamber (DCH), in a 1.5-T solenoidal field. The average vertex resolution in the $z$ direction is 70 $\mu$m for a fully reconstructed $B$ meson. We identify leptons and hadrons with measurements from all detector systems, including the energy loss ($\mathrm{d}E/\mathrm{d}x$) in the DCH and SVT. Electrons and photons are identified by a CsI electromagnetic calorimeter (EMC). Muons are identified in the instrumented flux return (IFR). A Cherenkov ring imaging detector (DIRC) covering the central region, together with the $\mathrm{d}E/\mathrm{d}x$ information, provides $K$-$\pi$ separation of at least three standard deviations for $B$ decay products with momentum greater than 250 MeV/$c$ in the laboratory.

We select events with a minimum of three reconstructed charged tracks, each having a laboratory polar angle between 0.41 and 2.54 rad and impact parameter in the plane transverse to the beam less than 1.5 cm from the beamline. The event must have a total measured energy in the laboratory greater than 4.5 GeV within the fiducial regions for charged tracks and neutral clusters. To help reject continuum background, the second Fox-Wolfram moment [8] must be less than 0.5.

An electron candidate must have a ratio of calorimeter energy to track momentum, an EMC cluster shape, a DCH $\mathrm{d}E/\mathrm{d}x$ and a DIRC Cherenkov angle (if available) consistent with an electron.

A muon candidate must satisfy requirements on the measured and expected number of interaction lengths penetrated, the position match between the extrapolated DCH track and IFR hits, and the average and spread of the number of IFR hits per layer.

A track is identified as a kaon candidate by means of a neural network that uses $\mathrm{d}E/\mathrm{d}x$ measurements in the DCH and SVT, and comparison of the observed pattern of detected photons in the DIRC with that expected for kaon and pion hypotheses.

Candidates for $J/\psi \to \ell^+\ell^-$ must have at least one decay product identified as a lepton (electron or muon) candidate or, if outside the calorimeter acceptance, must have DCH $\mathrm{d}E/\mathrm{d}x$ information consistent with the electron hypothesis. Tracks in which the electron has radiated are combined with bremsstrahlung photons, reconstructed as clusters with more than 30 MeV lying within 35 mr in polar angle and 50 mr in azimuth of the projected photon position on the EMC. The second track of a $\mu^+\mu^-$ pair, if within the acceptance of the calorimeter, must be consistent with being a minimum ionizing particle. Two identified electron or muon candidates are required for $J/\psi$ or $\psi(2S) \to \ell^+\ell^-$ reconstruction in the higher-background $\psi(2S)K_S^0$ and $J/\psi K_L^0$ channels.

We require a $J/\psi$ candidate to have $2.95 \le m_{e^+e^-} \le 3.14\,\mathrm{GeV}/c^2$ or $3.06 \le m_{\mu^+\mu^-} \le 3.14\,\mathrm{GeV}/c^2$, and a $\psi(2S) \to \ell^+\ell^-$ candidate to have $3.44 \le m_{e^+e^-} \le 3.74\,\mathrm{GeV}/c^2$ or $3.64 \le m_{\mu^+\mu^-} \le 3.74\,\mathrm{GeV}/c^2$. Requirements are made on the lepton helicity angle in order to provide further discrimination against background. For the $\psi(2S) \to J/\psi\pi^+\pi^-$ mode, mass-constrained $J/\psi$ candidates are combined with pairs of oppositely-charged tracks considered as pions; the resulting mass must be within 15 MeV/$c^2$ of the $\psi(2S)$ mass [4].

A $K_S^0 \to \pi^+\pi^-$ candidate must satisfy $489 < m_{\pi^+\pi^-} < 507\,\mathrm{MeV}/c^2$. The distance between the $J/\psi$ or $\psi(2S)$ and $K_S^0$ vertices is required to be at least 1 mm.

Pairs of $\pi^0$ candidates with total energy above 800 MeV are considered as $K_S^0$ candidates for the $J/\psi K_S^0$ mode. We determine the most probable $K_S^0$ decay point along the path defined by the initial $K_S^0$ momentum vector and the $J/\psi$ vertex by maximizing the product of probabilities for the daughter $\pi^0$ mass-constrained fits. Allowing for vertex resolution, we require the displacement from the $J/\psi$ vertex to the decay point to be between $-10$ and $+40$ cm and the $\pi^0\pi^0$ mass evaluated at this point to be between 470 and 550 MeV/$c^2$.

A $K_L^0$ candidate is formed from a cluster not matched to a reconstructed track. For the EMC the cluster must

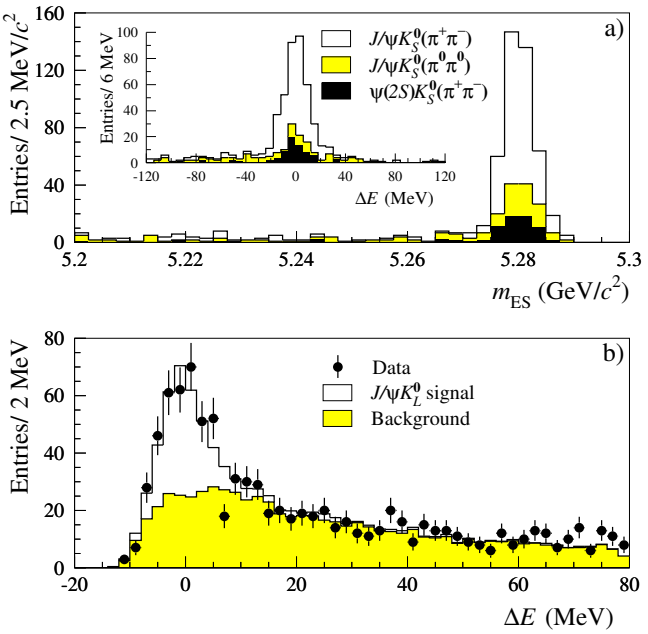


FIG. 1: a) Distribution of $m_{\rm ES}$ and $\Delta E$ for $B_{CP}$ candidates having a $K^0_S$ in the final state; b) distribution of $\Delta E$ for $J/\psi\, K^0_L$ candidates.

have energy above 200 MeV, while for the IFR the cluster must have at least two layers. We determine the $K^0_L$ energy by combining its direction with the reconstructed $J/\psi$ momentum, assuming the decay $B^0 \to J/\psi\, K^0_L$. To reduce photon backgrounds, EMC clusters consistent with a $\pi^0 \to \gamma\gamma$ decay are rejected and the transverse missing momentum of the event projected on the $K^0_L$ candidate direction must be consistent with the $K^0_L$ momentum. In addition, the center-of-mass $J/\psi$ momentum is required to be greater than 1.4 GeV/$c$.

$B_{CP}$ candidates used in the analysis are selected by requiring that the difference $\Delta E$ between the energy of the $B_{CP}$ candidate and the beam energy in the center-of-mass frame be less than three standard deviations from zero and that, for $K^0_S$ modes, the beam-energy substituted mass $m_{\rm ES} = \sqrt{(E^{\rm cm}_{\rm beam})^2 - (p^{\rm cm}_B)^2}$ falls in the interval $m_{\rm ES} > 5.2\,{\rm GeV}/c^2$. The resolution for $\Delta E$ is about 10 MeV, except for $J/\psi K^0_L$ (3 MeV) and the $K^0_S \to \pi^0\pi^0$ mode (33 MeV). For the purpose of determining numbers of events, purities and efficiencies, a signal region $m_{\rm ES} > 5.27\,{\rm GeV}/c^2$ is used for all modes except $J/\psi K^0_L$.

Figure 1 shows the resulting $\Delta E$ and $m_{\rm ES}$ distributions for $B_{CP}$ candidates containing a $K^0_S$, and $\Delta E$ for the candidates containing a $K^0_L$. The $B_{CP}$ sample is composed of 890 events in the signal region, with an estimated background of 260 events, predominantly in the $J/\psi K^0_L$ channel. For that channel, the composition, effective $\eta_f$ and $\Delta E$ distributions of the individual background sources are taken either from a Monte Carlo simulation (for $B$ decays to $J/\psi$) or the $m_{\ell^+\ell^-}$ sidebands in data.

For flavor tagging, we exploit information from the incompletely reconstructed other $B$ decay in the event. The charge of energetic electrons and muons from semileptonic $B$ decays, kaons, soft pions from $D^*$ decays, and high momentum charged particles is correlated with the flavor of the decaying $b$ quark: *e.g.*, a positive lepton yields a $B^0$ tag. Each event is assigned to one of four hierarchical, mutually exclusive tagging categories or is excluded from further analysis. The mistag fractions and efficiencies of all categories are determined from data.

A lepton tag requires an electron or muon candidate with a center-of-mass momentum $p_{\rm cm} > 1.0$ or 1.1 GeV/$c$, respectively. This efficiently selects primary leptons and reduces contamination due to oppositely-charged leptons from semileptonic charm decays. Events meeting these criteria are assigned to the `Lepton` category unless the lepton charge and the net charge of all kaon candidates indicate opposite tags. Events without a lepton tag but with a non-zero net kaon charge are assigned to the `Kaon` category.

All remaining events are passed to a neural network algorithm whose main inputs are the momentum and charge of the track with the maximum center-of-mass momentum, and the outputs of secondary networks, trained with Monte Carlo samples to identify primary leptons, kaons, and soft pions. Based on the output of the neural network algorithm, events are tagged as $B^0$ or $\overline{B}^0$ and assigned to the `NT1` (more certain tags) or `NT2` (less certain tags) category, or not tagged at all. The tagging power of the `NT1` and `NT2` categories arises primarily from soft pions and from recovering unidentified isolated primary electrons and muons.

Table I shows the number of tagged events and the signal purity, determined from fits to the $m_{\rm ES}$ ($K^0_S$ modes) or $\Delta E$ ($K^0_L$ mode) distributions. The measured efficiencies for the four tagging categories are summarized in Table II.

The uncertainty in the $\Delta t$ measurement is dominated by the measurement of the position $z_{\rm tag}$ of the tagging vertex. The tagging vertex is determined by fitting the tracks not belonging to the $B_{CP}$ (or $B_{\rm flav}$) candidate to a common vertex. Reconstructed $K^0_S$ and $\Lambda$ candidates are used as input to the fit in place of their daughters. Tracks from $\gamma$ conversions are excluded from the fit. To reduce contributions from charm decay, which bias the vertex estimation, the track with the largest vertex $\chi^2$ contribution greater than 6 is removed and the fit is redone until no track fails the $\chi^2$ requirement or fewer than two tracks remain. The average resolution for $\Delta z = z_{CP} - z_{\rm tag}$ is 190 $\mu$m. The time interval $\Delta t$ between the two $B$ decays is then determined from the $\Delta z$ measurement, including an event-by-event correction for the direction of the $B$ with respect to the $z$ direction in the $\Upsilon(4S)$ frame. An accepted candidate must have a converged fit for the $B_{CP}$ and $B_{\rm tag}$ vertices, an error of less than 400 $\mu$m on

TABLE I: Number of tagged events, signal purity and result of fitting for *CP* asymmetries in the full *CP* sample and in various subsamples, as well as in the $B_{\rm flav}$ and charged $B$ control samples. Purity is the fitted number of signal events divided by the total number of events in the $\Delta E$ and $m_{\rm ES}$ signal region defined in the text. Errors are statistical only.

| Sample | $N_{\rm tag}$ | Purity (%) | sin2$\beta$ |
|---|---|---|---|
| $J/\psi K^0_S$, $\psi(2S)K^0_S$ | 273 | $96 \pm 1$ | $0.25 \pm 0.22$ |
| $J/\psi K^0_L$ | 256 | $39 \pm 6$ | $0.87 \pm 0.51$ |
| Full *CP* sample | 529 | $69 \pm 2$ | $0.34 \pm 0.20$ |
| $J/\psi K^0_S$, $\psi(2S)K^0_S$ only | | | |
| $J/\psi K^0_S$ ($K^0_S \to \pi^+\pi^-$) | 188 | $98 \pm 1$ | $0.25 \pm 0.26$ |
| $J/\psi K^0_S$ ($K^0_S \to \pi^0\pi^0$) | 41 | $85 \pm 6$ | $-0.05 \pm 0.66$ |
| $\psi(2S)K^0_S$ ($K^0_S \to \pi^+\pi^-$) | 44 | $97 \pm 3$ | $0.40 \pm 0.50$ |
| `Lepton` tags | 34 | $99 \pm 2$ | $0.07 \pm 0.43$ |
| `Kaon` tags | 156 | $96 \pm 2$ | $0.40 \pm 0.29$ |
| `NT1` tags | 28 | $97 \pm 3$ | $-0.03 \pm 0.67$ |
| `NT2` tags | 55 | $96 \pm 3$ | $0.09 \pm 0.76$ |
| $B^0$ tags | 141 | $96 \pm 2$ | $0.24 \pm 0.31$ |
| $\overline{B}^0$ tags | 132 | $97 \pm 2$ | $0.25 \pm 0.30$ |
| $B_{\rm flav}$ sample | 4637 | $86 \pm 1$ | $0.03 \pm 0.05$ |
| Charged $B$ sample | 5165 | $90 \pm 1$ | $0.02 \pm 0.05$ |

TABLE II: Average mistag fractions $w_i$ and mistag differences $\Delta w_i = w_i(B^0) - w_i(\overline{B}^0)$ extracted for each tagging category $i$ from the maximum-likelihood fit to the time distribution for the fully-reconstructed $B^0$ sample ($B_{\rm flav}$+$B_{CP}$). The figure of merit for tagging is the effective tagging efficiency $Q_i = \varepsilon_i(1-2w_i)^2$, where $\varepsilon_i$ is the fraction of events with a reconstructed tag vertex that are assigned to the $i^{th}$ category. Uncertainties are statistical only. The statistical error on sin2$\beta$ is proportional to $1/\sqrt{Q}$, where $Q = \sum Q_i$.

| Category | $\varepsilon$ (%) | $w$ (%) | $\Delta w$ (%) | $Q$ (%) |
|---|---|---|---|---|
| `Lepton` | $10.9 \pm 0.4$ | $11.6 \pm 2.0$ | $3.1 \pm 3.1$ | $6.4 \pm 0.7$ |
| `Kaon` | $36.5 \pm 0.7$ | $17.1 \pm 1.3$ | $-1.9 \pm 1.9$ | $15.8 \pm 1.3$ |
| `NT1` | $7.7 \pm 0.4$ | $21.2 \pm 2.9$ | $7.8 \pm 4.2$ | $2.6 \pm 0.5$ |
| `NT2` | $13.7 \pm 0.5$ | $31.7 \pm 2.6$ | $-4.7 \pm 3.5$ | $1.8 \pm 0.5$ |
| All | $68.9 \pm 1.0$ | | | $26.7 \pm 1.6$ |

$\Delta z$ and a measured $|\Delta z| < 3\,$mm; 86% of the $B_{CP}$ events satisfy this requirement.

The sin2$\beta$ measurement is made with an unbinned maximum likelihood fit to the $\Delta t$ distribution of the combined $B_{CP}$ and $B_{\rm flav}$ tagged samples. The $\Delta t$ distribution of the former is given by Eq. 1, with $|\lambda| = 1$. The latter evolves according to the known rate for flavor oscillations in neutral $B$ mesons. The amplitudes for $B_{CP}$ asymmetries and for $B_{\rm flav}$ flavor oscillations are reduced by the same factor $(1-2w)$ due to mistags. The distributions are both convoluted with a common $\Delta t$ resolution function, and are corrected for backgrounds, incorporated with different assumptions about their $\Delta t$ evolution and convoluted with a separate resolution function. Events are assigned signal and background probabilities based on fits to $m_{\rm ES}$ (all modes except $J/\psi K^0_L$) or $\Delta E$ ($J/\psi K^0_L$) distributions.

The $\Delta t$ resolution function for signal candidates is represented by a sum of three Gaussian distributions with different means and widths. For the core and tail Gaussians, the widths are scaled by the event-by-event measurement error derived from the vertex fits; the combined rms is 1.1 ps. A separate offset for the core distribution is allowed for each tagging category to account for small shifts caused by inclusion of residual charm decay products in the tag vertex; a common offset is used for the tail component. The third Gaussian (of fixed 8 ps width) accounts for the fewer than 1% of events with incorrectly reconstructed vertices. Identical resolution function parameters are used for all modes, since the $B_{\rm tag}$ vertex precision dominates the $\Delta t$ resolution.

A total of 35 parameters are varied in the final fit, including the values of sin2$\beta$ (1), the average mistag fraction $w$ and the difference $\Delta w$ between $B^0$ and $\overline{B}^0$ mistags for each tagging category (8), parameters for the signal $\Delta t$ resolution (9), and parameters for background time dependence (6), $\Delta t$ resolution (3) and mistag fractions (8). The determination of the mistag fractions and signal $\Delta t$ resolution function is dominated by the high-statistics $B_{\rm flav}$ sample, while background parameters are governed by events with $m_{\rm ES} < 5.27\,{\rm GeV}/c^2$ (except $J/\psi K^0_L$). We fix $\tau_{B^0} = 1.548\,$ps and $\Delta m_{B^0} = 0.472\,\hbar\,{\rm ps}^{-1}$ [4]. The largest correlation between sin2$\beta$ and any linear combination of the other free parameters is 0.076.

The measurement of sin2$\beta$ was performed as a blind analysis by hiding the value of sin2$\beta$ obtained from the fit, as well as the *CP* asymmetry in the $\Delta t$ distribution, until the analysis was complete. This allowed us to study statistical and systematic errors without knowing the numerical value of sin2$\beta$.

The measured mistag rates obtained from the likelihood fit for the four tagging categories are summarized in Table II. As a check, the mistag rates were evaluated with a sample of about 16,000 $D^{*-}\ell^+\nu_\ell$ events and found to be consistent with the results from the hadronic decay sample.

The combined fit to the *CP* decay modes and the flavor decay modes yields

$$\sin2\beta = 0.34 \pm 0.20\ ({\rm stat}) \pm 0.05\ ({\rm syst}).$$

The decay asymmetry $A_{CP}$ as a function of $\Delta t$ and the log likelihood as a function of sin2$\beta$ are shown in Fig. 2. If $|\lambda|$ is allowed to float in the fit, the value obtained is consistent with 1 and there is no significant difference in the value of $-\eta_f\,\mathcal{I}m\,\lambda/|\lambda|$ (identified with sin2$\beta$ in the Standard Model) and our quoted result. Repeating the fit with all parameters fixed to their determined values except sin2$\beta$, we find a total contribution of $\pm 0.02$ to the error on sin2$\beta$ is due to the combined statistical uncertainties in mistag rates, $\Delta t$ resolution and background parameters.

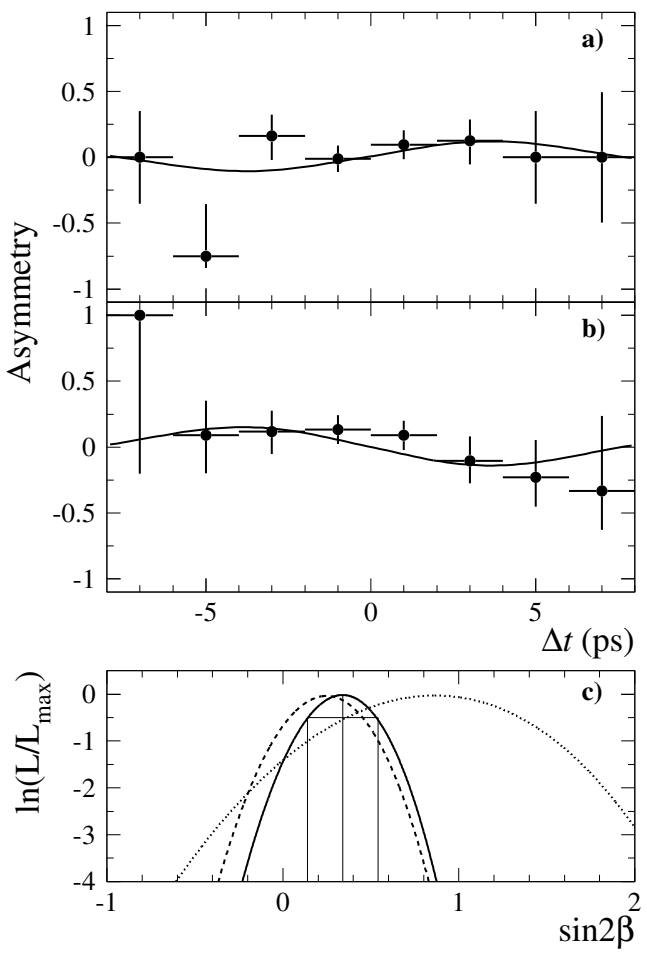


FIG. 2: The raw asymmetry in the number of $B^0$ and $\overline{B}^0$ tags in the signal region, $(N_{B^0} - N_{\overline{B}^0})/(N_{B^0} + N_{\overline{B}^0})$, with asymmetric binomial errors, as a function of $\Delta t$ for a) the $J/\psi\, K_S^0$ and $\psi(2S)K_S^0$ modes ($\eta_f = -1$) and b) the $J/\psi\, K_L^0$ mode ($\eta_f = +1$). The solid curves represent the time-dependent asymmetries determined for the central values of sin2$\beta$ from the fits for these samples. Eight events that lie outside the plotted interval were also used in the fits. The probability of obtaining a lower likelihood, evaluated using a Monte Carlo technique, is 60%. c) Variation of the log likelihood as a function of sin2$\beta$ for the modes containing $K_S^0$ (dashed curve), the $J/\psi\, K_L^0$ mode (dotted) and the entire sample (solid). For the latter, solid lines indicate the central value and values of the log likelihood corresponding to one statistical standard deviation.

The dominant sources of systematic error are the assumed parameterization of the $\Delta t$ resolution function (0.04), due in part to residual uncertainties in the SVT alignment, and uncertainties in the level, composition, and *CP* asymmetry of the background in the selected *CP* events (0.02). The systematic errors from uncertainties in $\Delta m_{B^0}$ and $\tau_{B^0}$ and from the parameterization of the background in the selected $B_{\rm flav}$ sample are found to be negligible. An increase of $0.02\,\hbar\,{\rm ps}^{-1}$ in the assumed value for $\Delta m_{B^0}$ decreases sin2$\beta$ by 0.012.

The large sample of reconstructed events allows a number of consistency checks, including separation of the data by decay mode, tagging category and $B_{\rm tag}$ flavor. The results of fits to these subsamples are shown in Table I for the high-purity $K_S^0$ events. Table I also shows results of fits with the samples of non-*CP* decay modes, where no statistically significant asymmetry is found.

Our measurement of sin2$\beta$ is consistent with, but improves substantially on the precision of, previous determinations [9]. The central value is consistent with the range implied by measurements and theoretical estimates of the magnitudes of CKM matrix elements [10]; it is also consistent with no *CP* asymmetry at the $1.7\sigma$ level.

We wish to thank our PEP-II colleagues for their extraordinary achievement in reaching design luminosity and high reliability in a remarkably short time. The collaborating institutions wish to thank SLAC for its support and the kind hospitality extended to them.

This work has been supported by the US Department of Energy and National Science Foundation, the Natural Sciences and Engineering Research Council (Canada), the Institute of High Energy Physics (China), Commissariat à l'Energie Atomique and Institut National de Physique Nucléaire et de Physique des Particules (France), Bundesministerium für Bildung und Forschung (Germany), Istituto Nazionale di Fisica Nucleare (Italy), the Research Council of Norway, the Ministry of Science and Technology of the Russian Federation, and the Particle Physics and Astronomy Research Council (United Kingdom). Individuals have received support from the Swiss National Foundation, the A. P. Sloan Foundation, the Research Corporation and the Alexander von Humboldt Foundation.

* Also with Università di Perugia, Perugia, Italy.
† Also with Università della Basilicata, Potenza, Italy.
‡ Deceased.

[1] A.B. Carter and A.I. Sanda, Phys. Rev. **D23**, 1567 (1981); I.I. Bigi and A.I. Sanda, Nucl. Phys. **B193**, 85 (1981).
[2] J.H. Christenson *et al.*, Phys. Rev. Lett. **13**, 138 (1964).
[3] See, for example, L. Wolfenstein, Eur. Phys. Jour. **C15**, 115 (2000).
[4] Particle Data Group, D.E. Groom *et al.*, Eur. Phys. Jour. **C15**, 1 (2000).
[5] N. Cabibbo, Phys. Rev. Lett. **10**, 531 (1963); M. Kobayashi and T. Maskawa, Prog. Th. Phys. **49**, 652 (1973).
[6] Throughout this paper, flavor-eigenstate decay modes imply also their charge conjugate.
[7] *BABAR* Collaboration, B. Aubert *et al.*, SLAC-PUB-8569, submitted to Nucl. Instr. and Methods.

[8] G.C. Fox and S. Wolfram, Phys. Rev. Lett. **41**, 1581 (1978).

[9] OPAL Collaboration, K. Ackerstaff *et al.*, Eur. Phys. Jour. **C5**, 379 (1998); CDF Collaboration, T. Affolder *et al.*, Phys. Rev. **D61**, 072005 (2000); ALEPH Collaboration, R. Barate *et al.*, Phys. Lett. **B492**, 259 (2000).

[10] See, for example, F.J. Gilman, K. Kleinknecht and B. Renk, Eur. Phys. Jour. **C15**, 110 (2000).